

# The cosmological principle is not in the sky

Chan-Gyung Park<sup>1</sup>, Hwasu Hyun<sup>2</sup>, Hyerim Noh<sup>3</sup> and Jai-chan Hwang<sup>2\*</sup>

<sup>1</sup>*Division of Science Education and Institute of Fusion Science, Chonbuk National University, Jeonju, Korea*

<sup>2</sup>*Department of Astronomy and Atmospheric Sciences, Kyungpook National University, Daegu, Korea*

<sup>3</sup>*Center for Large Telescope, Korea Astronomy and Space Science Institute, Daejeon, Korea*

The homogeneity of matter distribution at large scales is a central *assumption* in the standard cosmological model. The case is testable though, thus no longer needs to be a principle, and indeed there have been claims that the distribution of galaxies is homogeneous at radius scales larger than  $70 h^{-1}\text{Mpc}$ . Here we perform a test for homogeneity using the Sloan Digital Sky Survey Luminous Red Galaxies (LRG) sample by counting galaxies within a specified volume with the radius scale varying up to  $300 h^{-1}\text{Mpc}$ . Our analysis differs from the previous ones in that we directly confront the large-scale structure data with the definition of spatial homogeneity by comparing the *fluctuations* of individual number counts with allowed ranges of the *random* distribution with homogeneity. The LRG sample shows much larger fluctuations of number counts than the random catalogs up to  $300 h^{-1}\text{Mpc}$  scale, and even the average is located far outside the range allowed in the random distribution, which implies that the cosmological principle does not hold even at such large scales. The same analysis of mock galaxies derived from the  $N$ -body simulation, however, suggests that the LRG sample is consistent with the current paradigm of cosmology. Thus, we conclude that the cosmological principle is not in the observed sky and nor is demanded to be there by the standard cosmological world model. This reveals the nature of the cosmological principle adopted in the modern cosmology paradigm, and opens new field of research in theoretical cosmology.

*Introduction.* The modern physical cosmology is built on a simple geometrical *assumption* about distribution of matter in the large-scale [1]. The cosmological principle (CP) of modern cosmology states that spatial distribution of matter is homogeneous and isotropic in the large-scale. Being a statement on physical state of matter, it is testable using the observed redshift and the angular location in the sky of luminous galaxies; the distance is not directly available and in cosmology we have to consider that different distances correspond to different temporal epochs in the history of the universe. The physical state of distribution of course cannot be exactly homogeneous and isotropic which is merely a mathematical idealization. In practice however one can *test* the assumption by comparing the distribution with the random one. As we know that the small scale distributions of celestial objects are apparently far from homogeneous or isotropic, we can anticipate that if the CP is true there might appear a homogeneity-scale (HS) above which the distribution is statistically indistinguishable from the random one. Our aim in this *Letter* is to find out the HS from observation.

Such studies based on galaxy count are available in the literature and there are several claims about the HS reached at scales of  $70\text{--}100 h^{-1}\text{Mpc}$  [2–8] (see [9, 10] for somewhat larger HS);  $h$  is the Hubble parameter normalized to  $100 \text{ km s}^{-1}\text{Mpc}^{-1}$ ; for contrary views, see [11–13]. We find, however, most of the methods used to reach the conclusion are not about direct test one can naïvely think of, i.e., comparing the fluctuations in the galaxy counts with the one in the *random* realization. Our result based on such a method shows that even far beyond the claimed HS the observed distribution is *not* homogeneous even at  $300 h^{-1}\text{Mpc}$  scales! This is true not only for fluctuations but also for average as well. Therefore, our conclusion is that the observation we have used does *not* show any HS.

Our conclusion does not necessarily imply that the current cosmological paradigm is challenged. Although the modern cosmology is fundamentally based on the CP, it is a *theoretical* assumption on a *fictional* background. In a realistic case the background model should be added by small-amplitude (about  $2 \times 10^{-5}$  dimensionless level in the early epoch) perturbations in all scales, and the background can be achieved by spatial averaging. Due to the gravitational instability the fluctuations are amplified in time especially from the small scales. Thus, as long as the consequent theoretically predicted fluctuations are consistent with the observation the cosmological paradigm based on CP in the background universe (in the early era) is safe independently of the strong statement on the actual existence of CP in the observed sky; without the HS the CP in that space (even in a background) lose its meaning.

Although the issue on whether or not the colossal structures discovered in the large-scale, like the Sloan Digital Sky Survey (SDSS) Great Wall boasting  $300 h^{-1}\text{Mpc}$  in linear dimension, is consistent with the cosmological simulation is currently under debate [14], our additional test in this work, now comparing observation with the simulation, reveals that the observed fluctuations are *consistent* with the simulated ones at radius scales up to  $300 h^{-1}\text{Mpc}$ . Thus, we may conclude that although we do not have the HS in the observed galaxy distribution, the modern cosmology theoretically based on the CP is consistent with the observed large-scale galaxy distribution.

In this *Letter*, we perform a direct test for homogeneity of large-scale structure using the recent galaxy redshift survey data by counting galaxies within a specified volume with varying size scale. Unlike the previous studies based on the *average trend* of galaxy counts over differ-

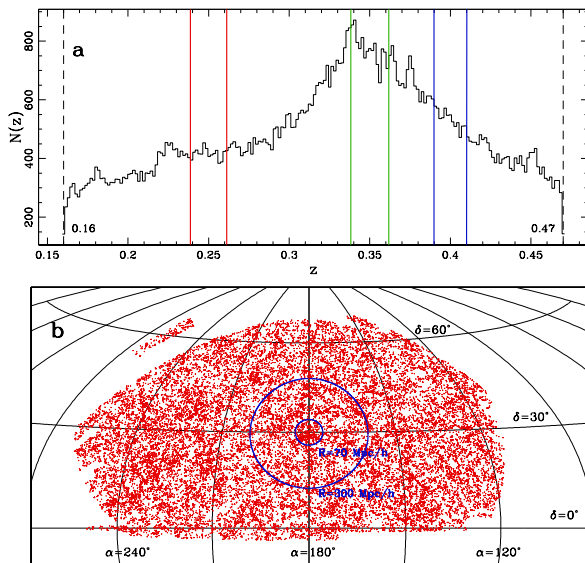


FIG. 1: **Redshift (a) and angular (b) distributions of the SDSS LRG.** In **a**, vertical lines denote three redshift slices of  $50 h^{-1}\text{Mpc}$  thickness centered at  $z_c = 0.25, 0.35,$  and  $0.40$ . In **b**, angular distribution is shown for galaxies within a slice with thickness of  $140 h^{-1}\text{Mpc}$  centered at  $z_c = 0.35$  in the Hammer-Aitoff equal-area projection with equatorial coordinates. Circles with the claimed HS ( $70 h^{-1}\text{Mpc}$ ) and  $300 h^{-1}\text{Mpc}$  as radius are shown for a comparison.

ent scales, our analysis compares the *fluctuations* (in addition to the average) of individual number counts with the expected range allowed by the random distribution with homogeneity.

*SDSS Luminous Red Galaxies.* We use the SDSS Data Release 7 Luminous Red Galaxies (LRG) sample [15, 16] to explore the homogeneity of our local universe. The LRG sample contains galaxies that are believed to be a good tracers of massive halos, and quasi-volume-limited up to redshift  $z \simeq 0.36$ , thereafter flux-limited up to  $z \simeq 0.47$ . We use the LRG sample provided in [17], which includes 105,831 galaxies over redshift range of  $0.16 < z < 0.47$  with effective volume of  $1.6 h^{-3}\text{Gpc}^3$  (see Fig. 1).

*Random catalogs and Mock catalogs.* In order to decide whether or not the LRG are homogeneously distributed at a given scale, we compare the galaxy counts with those from homogeneous distribution. For this purpose, we generate 1,000 random catalogs, each containing the Poisson-distributed data points with the same number as in the LRG sample, by considering LRG redshift distribution and angular selection function as the probability functions. We analyze these catalogs to set the criterion for the spatial homogeneity.

We also make the mock catalogs that mimic the LRG sample. Using the all-sky lightcone halo catalogs made from  $N$ -body simulation [18], we generate 1,296 LRG mock data sets, with individual survey area uniformly separated but significantly overlapped on the sky. Within

the survey area, massive halos with the same number of LRG have been extracted in decreasing order of halo mass by considering the LRG redshift distribution and angular selection function (see Methods for details). We analyze these mock data sets to check whether or not the observation is consistent with the current paradigm of cosmology.

*Counting galaxies within a sphere.* To test for homogeneity of large-scale structure, first we apply the count-in-sphere method in the similar way as in [2]. As a measure of homogeneity, we calculate the scaled count-in-sphere  $\mathcal{N}(R)$  defined as the number of galaxies within a sphere of comoving radius  $R$  centered at each galaxy divided by the number expected in the homogeneous distribution. The latter is estimated from a random point distribution which contains 100 times larger number of data points than the single data set. For each  $\mathcal{N}(R)$ , we assign a weight which is a fraction of the volume of a sphere within the survey relative to that of a complete sphere (volume-incompleteness).

Figure 2a–d show the weighted average of the scaled counts for comoving radius up to  $300 h^{-1}\text{Mpc}$  and histograms of individual  $\mathcal{N}$ 's for three chosen radii. The averaged  $\mathcal{N}$  goes over into unity with a flat slope at scales larger than around  $70 h^{-1}\text{Mpc}$ , approaching to  $\mathcal{N} = 1$  within 1% at  $R = 300 h^{-1}\text{Mpc}$ , which is very similar to the results shown in [2] and used to imply the existence of claimed HS. However, individual scaled counts show significant fluctuations deviating from the average. The scatter decreases as the radius increases with standard deviations of 0.17 (0.05), 0.08 (0.02) and 0.05 (0.01) for the LRG (one random) catalog at  $R = 100, 200$  and  $300 h^{-1}\text{Mpc}$ , respectively. Thus, the LRG sample has 5 times larger fluctuations even at  $300 h^{-1}\text{Mpc}$ .

We emphasize that *fluctuations* are more important measure of the homogeneity than the approaching of *average* numbers to the homogeneous ones; the latter is only one of the necessary conditions for homogeneity. Later we will show that even the average of the LRG (while consistent with mock data) show statistically significant deviation from the random one.

*Counting galaxies within redshift ranges.* The count-in-sphere method needs the random point distribution to correct for the bias due to the survey incompleteness in radial (thus time) direction. Here we apply a count-in-redshift-range method which avoids such a bias without the need to use the random distribution. In order to save computation time we consider a truncated cone instead of a sphere. We select LRG within a slice of  $50 h^{-1}\text{Mpc}$  thickness at the central redshift  $z_c$ . In our analysis three slices are chosen with  $z_c = 0.25, 0.35,$  and  $0.40$  (Fig. 1a). For each galaxy within the thin slice, we place a sphere of radius  $R$  at  $z_c$  but with the galaxy's angular position, and define a truncated cone that is circumscribed about the sphere. The upper and base sides of the truncated cone set the minimum and maximum redshifts ( $z_1$  and  $z_2$ ) which determine the slice of  $z_2 - z_1$  (or  $2R$ ) thickness. Then, we count galaxies within the truncated cone

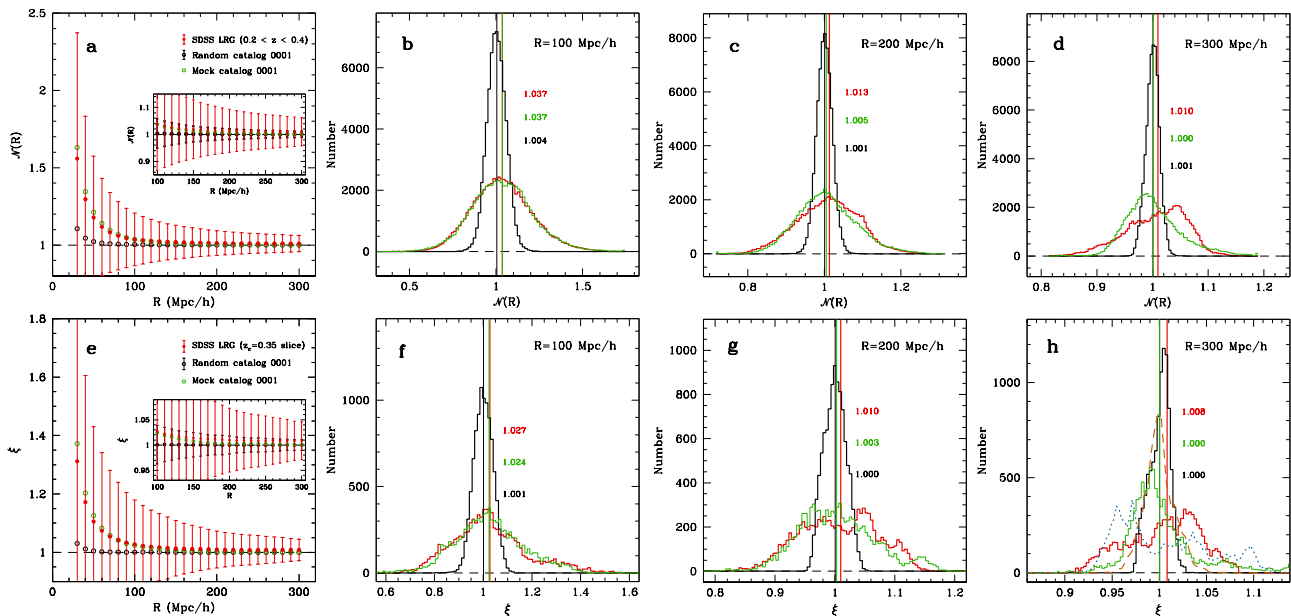


FIG. 2: **Results of counting galaxies over varying size scales.** (a) The weighted average of the scaled counts-in-sphere  $\mathcal{N}(R)$  versus  $R = 30\text{--}300 h^{-1}\text{Mpc}$ , estimated from the LRG at  $0.2 < z < 0.4$  (red dots with error bars). Black and green circles indicate results for one of the random and mock catalogs, respectively. The error bars for the LRG and a random catalog are compared in the small panel. (b–d) Histograms of individual  $\mathcal{N}$ 's at  $R = 100, 200,$  and  $300 h^{-1}\text{Mpc}$ , with the same color code. Vertical lines with numbers (from top to bottom) indicate the average of  $\mathcal{N}$ 's from the LRG, mock and random catalogs. (e–h) The same as a–d but for  $\xi$  measurements for the LRG within the  $z_c = 0.35$  slice. For  $R = 300 h^{-1}\text{Mpc}$  in h, the blue dotted and brown dashed curves indicate the results for the mock catalogs having the maximum and minimum fluctuations in the  $\xi$ -distribution, respectively (see Figs. 3c–d and 4f).

and calculate a new measure of homogeneity  $\xi$  defined as the number density of galaxies within a truncated cone divided by that within the whole slice. For a homogeneous distribution, we expect  $\xi$  to approach unity compared with the random distribution at scales larger than HS. Each  $\xi$  is assigned a weight that is the volume-incompleteness of a truncated cone. Figure 2e–h show the weighted average of  $\xi$ 's versus  $R$  for  $z_c = 0.35$  slice galaxies, together with histograms of individual  $\xi$ 's for three chosen radii.

As in the case of count-in-sphere, the LRG histograms from the count-in-redshift-range analysis confirm that the averaged  $\xi$  seems to approach homogeneity with 1% accuracy at  $300 h^{-1}\text{Mpc}$  scale. However, individual  $\xi$ 's show significant fluctuations far deviating from the range allowed by the random catalogs with homogeneous distribution. The unstable behaviors of fluctuations for LRG and mock data at  $300 h^{-1}\text{Mpc}$  scale also suggest that the homogeneity has not been reached yet at such a scale (Fig. 2h). This is visually demonstrated in Fig. 3 where  $\xi$  has been estimated on pixelized positions within the survey area for the LRG, one random, two mock catalogs with the maximum and minimum fluctuations in  $\xi$  measurements.

*Discussion.* In this *Letter*, we directly confront the large-scale structure data with the definition of spatial homogeneity by considering that beyond the HS there would be no variation in the galaxy counts within the

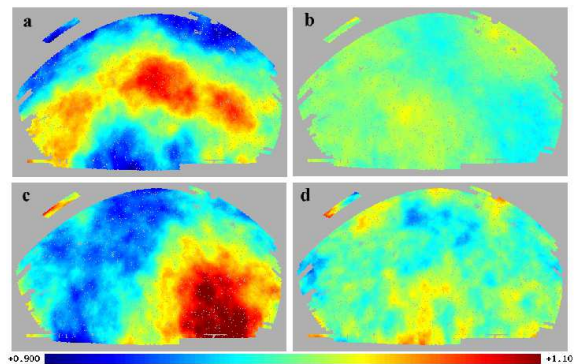


FIG. 3: **Angular distributions of  $\xi$ .** Shown are  $\xi$  maps for the  $z_c = 0.35$  slice at  $R = 300 h^{-1}\text{Mpc}$  scale estimated from (a) the LRG, (b) one random, and mock catalogs with (c) the maximum and (d) minimum fluctuations in  $\xi$  measurements; locations of b–d in a statistics plot are indicated as grey symbols in Fig. 4f. The corresponding angular distributions of data points are shown in Extended Data Fig. 1.

scatter expected in the Poisson distribution. The two galaxy-counting methods we adopted have a limitation that  $\mathcal{N}$  (or  $\xi$ ) goes over into unity on the survey-sized scale regardless of whether or not homogeneity has been reached [3]. However, for a distribution with HS smaller than the survey size the  $\mathcal{N}$  and  $\xi$  should approach unity at all scales beyond HS within the precision allowed by

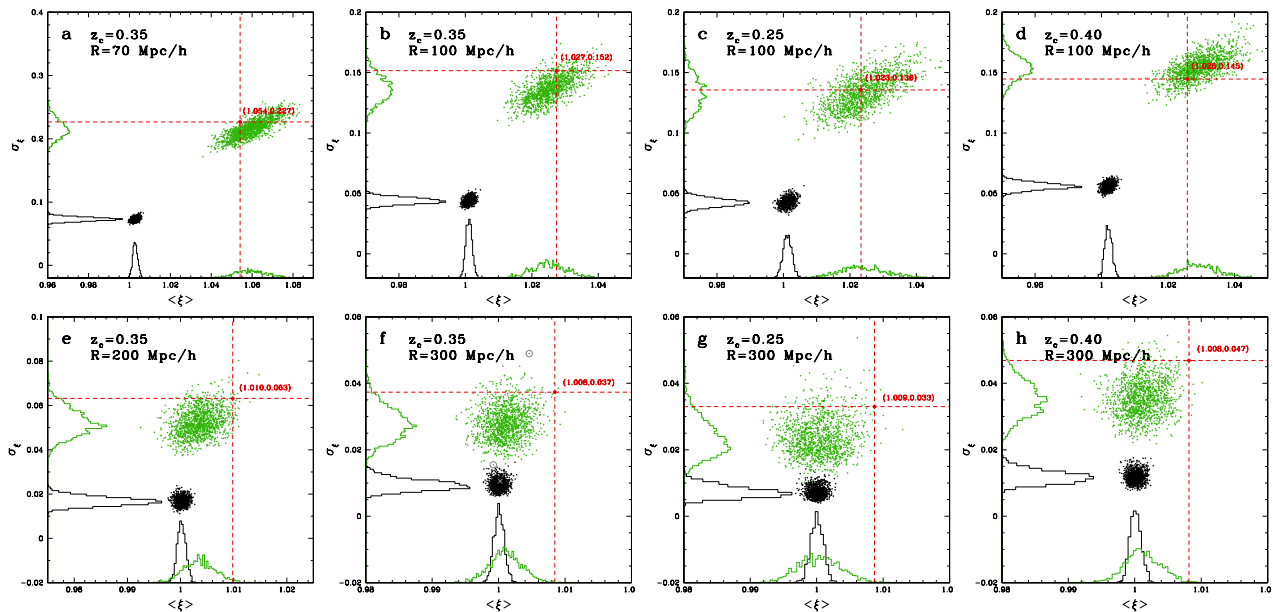


FIG. 4: Plots of  $\langle \xi \rangle$  versus  $\sigma_\xi$ . Results for the  $z_c = 0.35$  slice at  $R = 70, 100, 200, 300 h^{-1}\text{Mpc}$  are shown in **a, b, e, f**, respectively, estimated from the LRG (red dots with dotted lines and numbers), 1,000 random (black), and 1,296 mock catalogs (green dots), with the corresponding histograms shown on the axes. In **f**, grey symbols indicate the random catalog and two mock catalogs (with the maximum and minimum  $\sigma_\xi$ ) that were chosen to present Fig. 3**b-d**. **c-d** and **g-h** present the results for  $z_c = 0.25$  and  $0.40$  slices at  $R = 100$  and  $300 h^{-1}\text{Mpc}$ , respectively.

the random catalogs. Our analyses demonstrate that the LRG distribution does *not* show homogeneity at the claimed HS that was usually determined based on the average trend of galaxy number count with increasing scale [2–4].

To quantify the significance of the deviation from homogeneity, we compare the average  $\langle \xi \rangle$  and standard deviation  $\sigma_\xi$  estimated from the  $\xi$ -distribution for the LRG, random, and mock catalogs. As shown in Fig. 4, the LRG sample and most of mock catalogs significantly deviate from the range allowed by the random distribution with spatial homogeneity at  $70\text{--}300 h^{-1}\text{Mpc}$  scales (**a-b, e-f**) and the behavior persists over different redshifts (**b-d, f-h**) for both fluctuations and averages. At  $z_c = 0.35$  and  $R = 300 h^{-1}\text{Mpc}$  (**f**), the deviations are  $11\sigma$  and  $17\sigma$  for  $\langle \xi \rangle$  and  $\sigma_\xi$ , respectively; this means statistically *impossible* to be realized in the random distribution. Note that the deviation becomes larger at smaller scales.

The mock catalogs also show larger fluctuations in both  $\langle \xi \rangle$  and  $\sigma_\xi$  than the random ones, which is another evidence for the fact that the  $N$ -body clustering is no longer homogeneous even at  $300 h^{-1}\text{Mpc}$  scales. The LRG results also seem to somewhat deviate from the mock results at large scales ( $3.0\sigma$  for  $\langle \xi \rangle$  and  $1.9\sigma$  for  $\sigma_\xi$ ; Fig. 4**f**). Considering the dense overlaps of survey areas of mock catalogs, however, we can expect that the scatters in  $\xi$  statistics become larger for independent mock samples. In this sense, the LRG deviations are allowed to occur statistically. Figure 4**b-d** shows that in the  $\langle \xi \rangle$ - $\sigma_\xi$  plane the three independent LRG data can occur in arbitrary location of the region occupied by the

mock data; the similar locations of the LRG data for  $R = 300 h^{-1}\text{Mpc}$  in Fig. 4**f-h** are due to severe overlapping of the LRG data in the redshift direction for such a huge radius. Therefore, we conclude that the LRG distribution is consistent with the current paradigm of cosmology.

*Conclusion.* The large-scale structure shown in the SDSS LRG sample is not spatially homogeneous even at  $300 h^{-1}\text{Mpc}$  scale in radius, substantially deviating from the expected distribution with homogeneity, see Fig. 4. For LRG data there is no HS found yet. Therefore, the claimed HS at  $70 h^{-1}\text{Mpc}$  based on similar data [2] is disputed. To determine the value of HS (if it exists), it is essential to analyze data with larger survey volume;  $300 h^{-1}\text{Mpc}$  is near maximal radius scale available in the LRG data especially in the redshift direction. We defer the analysis with more recent data (e.g., SDSS-III BOSS survey [19]) for future work.

If the CP is not in the sky, where is it then in the Universe? The current concordance cosmology theoretically based on the CP in the *early* era is generally accepted to be quite successful in explaining most of the cosmological observations. Our homogeneity test shows that the model prediction is also consistent with the observation. If that is the case the CP may stay in the theoretical foundation of the modern physical cosmology (in the early era), but not in the sky (i.e., in the present epoch). That is, the celebrated modern cosmology paradigm does not demand the actual presence of CP in our observed sky. This conclusion opens a new possibility in theoretical cosmology demanding careful study of light propagation in



nonlinear clustering stage of the world model [20].

*Acknowledgements.* C.G.P. was supported by Basic Science Research Program through the National Research Foundation of Korea (NRF) funded by the Ministry of Science, ICT and Future Planning (No. 2013R1A1A1011107). H.N. was supported by NRF funded by Ministry of Science, ICT and Future Planning (No. 2015R1A2A2A01002791). J.H. was supported by Basic Science Research Program through the NRF of Korea funded by the Ministry of Science, ICT and Future Planning (No. 2013R1A2A2A01068519 and No. 2016R1A2B4007964).

*Author Contributions.* C.G.P. and H.H. performed data analysis. All authors contributed to the interpretation of the data and the discussion of the results. C.G.P., H.N. and J.H. contributed to writing the paper.

*Author Information.* The authors declare no competing financial interests. Correspondence should be addressed to J.H. (jchan@knu.ac.kr).

## Methods

*The SDSS LRG sample.* We use the non-official SDSS LRG sample [17] which can be obtained from the internet link, <http://cosmo.nyu.edu/~eak306/SDSS-LRG.html>. Although the SDSS LRG sample is smaller in galaxy number and survey volume than the recent galaxy surveys, it is still useful for homogeneity test due to two reasons. First, we can compare our result with the previous ones obtained with the same sample [2]. Second, since there is a claimed HS at  $70 h^{-1}\text{Mpc}$  scales that is far smaller than the LRG survey size, the larger sample of galaxies is not needed to draw a counter result. The sample is composed of luminous galaxies selected from the SDSS seventh and final data release (DR7) [15], and is found to be in agreement with the official LRG sample [17].

Here, the full DR7 LRG sample with redshift  $0.16 < z < 0.47$  and  $g$ -band absolute magnitude range of  $-23.2 < M_g < -21.2$  has been used. In Fig. 1b, we have applied the Hammer-Aitoff equal-area projection [21] to plot 26,285 galaxies on the sky. Given right ascension ( $\alpha$ ) and declination ( $\delta$ ) in equatorial coordinates, the projection onto  $(x, y)$ -plane is defined as

$$x = 2\gamma \cos\left(\frac{\alpha}{2}\right) \cos\delta, \quad y = \gamma \sin\delta \quad (1)$$

where

$$\gamma = \left( \frac{2}{1 + \sin\left(\frac{\alpha}{2}\right) \cos\delta} \right)^{1/2}. \quad (2)$$

As well as the angular position and redshift, the LRG sample also contains the additional information for each galaxy such as the sector incompleteness ( $w_s$ ) and the fiber collision weight ( $w_f$ ). For usual galaxies, the unit value of the fiber collision weight is assigned ( $w_f = 1$ ).

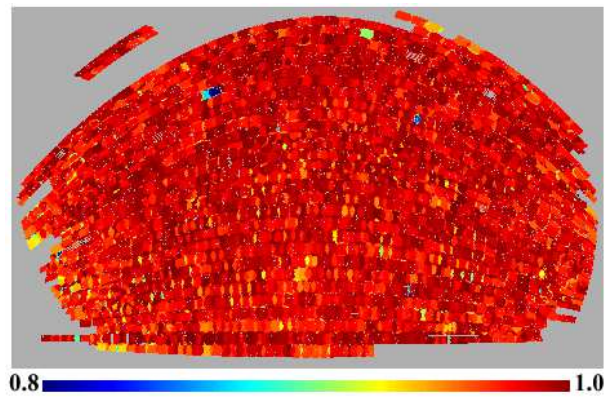


FIG. 5: **Angular selection function of the SDSS DR7 LRG sample.** The color indicates the sector incompleteness ( $w_s$ ).

Sometimes target galaxies are separated by less than  $55''$ , the angular diameter covered by the spectroscopic fiber, and they cannot be observed simultaneously due to fiber collision. In such cases, only one galaxy has the priority for spectroscopic observation and the fiber collision weight larger than unity is assigned ( $w_f > 1$ ) [22].

*Reconstructing angular selection function.* The observation of SDSS galaxy redshift survey has not been performed uniformly within the survey region due to several reasons. The survey region is composed of overlapping tiles and masked area due to bright stars and objects, fiber priority, bad fields, and so on. A unique set of tiles covering any area of sky is called a sector, and each sector is assigned the sector incompleteness determined by the fraction of galaxies with the successful spectroscopic observation relative to the total objects within the sector.

Here, the survey incompleteness in angular direction (angular selection function) is reconstructed using the sector incompleteness information contained in the random point distribution with 1.7 million data points provided in [17] (Fig. 5). In representing the angular selection function on the sky, we use the HEALpix software [23] which provides the equal-area pixelization on the sky with the total number of pixels  $N_{\text{pix}} = 12N_{\text{side}}^2$ , where  $N_{\text{side}}$  is the resolution parameter.  $N_{\text{side}} = 2048$  is sufficient for our purpose of mapping the angular selection function.

*Generating random and mock catalogs.* In order to establish the criterion for the spatial homogeneity, it is essential to generate the random catalogs, each containing the Poisson-distributed data points. A random catalog is generated as follows. First, a redshift  $z$  is randomly drawn in the range  $0.16 \leq z \leq 0.47$  with a probability function shown in Fig. 1a. Second, angular position ( $\alpha, \delta$ ) on the sky is randomly drawn using the angular selection function map (Fig. 5) as the probability function. Each random data point is assigned the sector incompleteness ( $w_s$ ). For simplicity, we assign the uniform fiber collision weights to all the random points ( $w_f = 1$ ). In this way,

we generate a random point catalog which includes the same number of galaxies as in the LRG sample, and 1,000 random catalogs in total.

The mock catalogs mimicking the LRG sample are generated in a similar way. The Horizon Run 3  $N$ -body simulation was made using 374 billion particles in a volume of  $(10.815 h^{-1}\text{Gpc})^3$ , which allows to resolve galaxy-size halos with mean particle separation of  $1.5 h^{-1}\text{Mpc}$  [18]. A set of 27 all-sky mock surveys (designed for SDSS-III) along the past lightcone out to  $z = 0.7$  is publicly available (<http://sdss.kias.re.kr/astro/Horizon-Runs/Horizon-Run23.php>). The cosmological model used in the simulation is the  $\Lambda$  cold dark matter ( $\Lambda\text{CDM}$ ) dominated universe with  $\Omega_M = 0.26$ ,  $\Omega_B = 0.044$ ,  $\Omega_\Lambda = 0.74$ ,  $n_s = 0.96$ ,  $h = 0.72$ , and  $\sigma_8 = 0.79$ , where  $\Omega_M$ ,  $\Omega_B$ ,  $\Omega_\Lambda$  are the current matter, baryon, dark energy density parameters, respectively,  $n_s$  the spectral index of primordial scalar-type perturbation,  $\sigma_8$  the amplitude of the matter fluctuations at  $8 h^{-1}\text{Mpc}$  scale. The angular positions of the survey center are chosen based on the HEALpix pixelization of  $N_{\text{side}} = 2$ . Thus, for each halo catalog, 48 LRG mock catalogs are generated with individual survey area significantly overlapped on the sky, and  $27 \times 48 = 1296$  catalogs are made in total. In the LRG mock survey, we also assign the sector incompleteness ( $w_s$ ) to each halo and the uniform fiber collision weights to all the data points ( $w_f = 1$ ).

*Counting galaxies within a sphere.* We assume  $\Lambda\text{CDM}$  dominated universe to calculate the comoving distance to a galaxy at redshift  $z$

$$r(z) = \frac{c}{H_0} \int_0^z \frac{dz}{\sqrt{\Omega_M(1+z)^3 + \Omega_\Lambda}}, \quad (3)$$

where  $c$  is the speed of light and  $H_0$  is Hubble's constant. We assume  $\Omega_M = 0.27$  and  $\Omega_\Lambda = 0.73$ . Given a sphere of comoving radius  $R$  at redshift  $z$  or at distance  $r_0 = r(z)$ , the angular radius of the sphere on the sky is given by  $\theta_R = \sin^{-1}(R/r_0)$ . We count galaxies within the sphere from the LRG sample and compare the number count with that expected from the homogeneous distribution. Each galaxy contributes  $w_f/w_s$  to the galaxy number counts. The random point distribution with 100 times larger number of points than the LRG catalog is needed to estimate the expected number of galaxies within a sphere. Each random point contributes  $0.01w_f/w_s$  to the count. The scaled  $\mathcal{N}(R)$  is obtained from the sum of all the LRG contributions divided by that of random point distribution within the sphere of radius  $R$ .

In estimating the weighted average and standard deviation of the scaled  $\mathcal{N}$ 's, the volume-incompleteness is used as the weight. The volume-incompleteness for each

measured  $\mathcal{N}$  is obtained by comparing the volume of the sphere contained within the survey region with that of a complete sphere, centered at the location of a galaxy. The volume of a sphere is estimated by summing the volume elements over the direction of HEALpix pixels with  $N_{\text{side}} = 2048$  penetrating the sphere. The distances to the near and far ends of the penetrating line are

$$r_{\pm} = r_0 \left[ \cos \theta \pm \sqrt{\sin^2 \theta_R - \sin^2 \theta} \right] \quad (4)$$

where  $\theta$  is the angular separation between the center of a sphere and a line-of-sight direction penetrating the sphere. The volume element for each pixel is given by

$$v_{\text{pix}} = \frac{\Omega_{\text{pix}}}{3} (r_+^3 - r_-^3) \quad (5)$$

where  $\Omega_{\text{pix}} = 4\pi/N_{\text{pix}}$ . The total volume of the sphere is the sum of all the volume elements within the survey region. Sometimes, the sphere is cut off by the survey boundary at the minimum/maximum distance ( $r_{\text{min}}/r_{\text{max}}$ ) from us. In that cases, we set  $r_- = r_{\text{min}}$  or  $r_+ = r_{\text{max}}$ .

*Counting galaxies within a truncated cone.* In the  $\xi$  measurement, the count-in-redshift-range method does not need to use the random point distribution. The method estimates only the number density of galaxies within the truncated cone and within the whole slice which is determined by the redshift range ( $z_1 < z < z_2$ ) set by the upper and base sides of the truncated cone. As in the count-in-sphere method, we consider the sector incompleteness and the fiber collision weight in counting the galaxies. For volume-incompleteness of the truncated cone, we estimate the volume contained within the survey region using the method used in the case of count-in-sphere. However, in this case the  $r_-$  and  $r_+$  are comoving distances to  $z_1$  and  $z_2$ , respectively, for a given central redshift  $z_c$  and the scale radius  $R$ . The volume of the complete truncated cone is given by

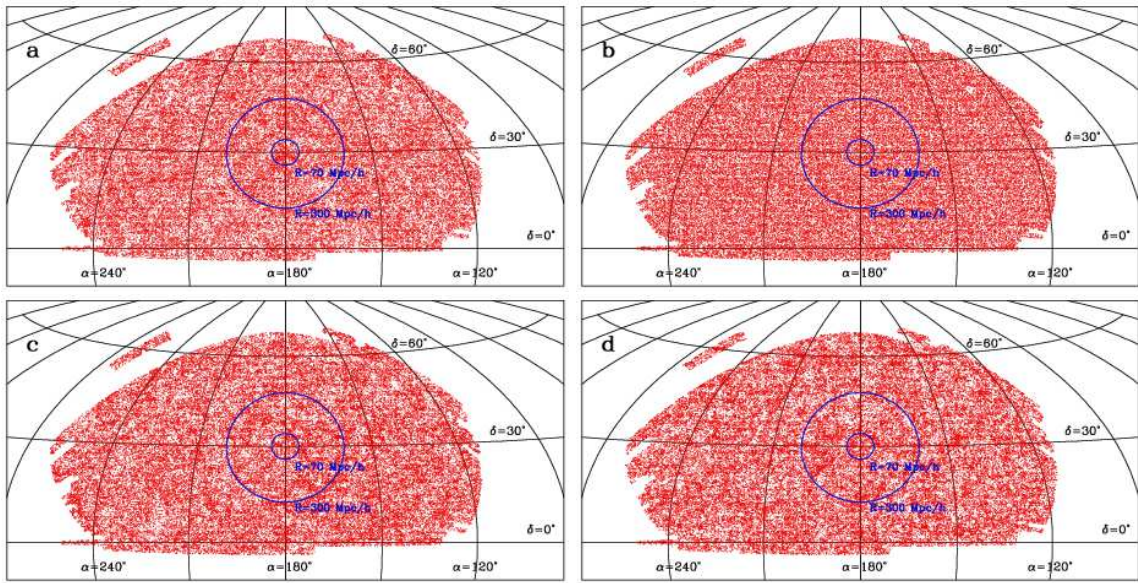
$$V_{\text{trc}} = \frac{4\pi}{3} (r_+^3 - r_-^3) \sin^2 \left( \frac{\theta_R}{2} \right). \quad (6)$$

*Generating  $\xi$ -maps.* The measurement of  $\xi$  has been done at the slice center and angular position of each data point in the LRG, random, and mock samples. In the  $\xi$ -maps shown in Fig. 3, however, we calculate  $\xi$  at angular positions centered on HEALPix pixels (with  $N_{\text{side}} = 256$ ) within the survey region in order to obtain the continuous maps. Other details are exactly the same as in the method described in the text.

---

[1] A. Einstein, "Kosmologische Betrachtungen zur allgemeinen Relativitätstheorie," Sitzungsab. Preuss. Akad.

Wiss., **1917**, 142 (1917).



**Extended Data Fig. 1.** Angular distributions of data points at  $0.235 < z < 0.470$  for (a) the SDSS LRG, (b) one random, and mock catalogs with (c) the maximum and (d) minimum fluctuations. Each distribution corresponds to the slice defined by the central redshift  $z_c = 0.35$  and the thickness of  $2R = 600 h^{-1}\text{Mpc}$ . The slice has been a bit cut off by the survey boundary at the maximum distance ( $z = 0.47$ ). Corresponding maps of  $\xi$  are presented in Fig. 3.

- [2] D.W. Hogg, D.J. Eisenstein, M.R. Blanton, N.A. Bahcall, J. Brinkmann, J.E. Gunn and D. P. Schneider, “Cosmic homogeneity demonstrated with luminous red galaxies,” *Astrophys. J.* **624**, 54 (2005).
- [3] M.I. Scrimgeour, T. Davis, C. Blake *et al.*, “The WiggleZ Dark Energy Survey: the transition to large-scale cosmic homogeneity,” *Mon. Not. Roy. Astron. Soc.* **425**, 116 (2012).
- [4] P. Ntelis, “The Homogeneity Scale of the universe,” arXiv:1607.03418 [astro-ph.CO].
- [5] J. Yadav, S. Bharadwaj, B. Pandey and T.R. Seshadri, “Testing homogeneity on large scales in the Sloan Digital Sky Survey Data Release One,” *Mon. Not. R. Astron. Soc.* **364**, 601 (2005).
- [6] J.S. Bagla, J. Yadav and T.R. Seshadri, “Fractal Dimensions of a Weakly Clustered Distribution and the Scale of Homogeneity,” *Mon. Not. Roy. Astron. Soc.* **390**, 829 (2007).
- [7] P. Sarkar, J. Yadav, B. Pandey and S. Bharadwaj, “The scale of homogeneity of the galaxy distribution in SDSS DR6,” *Mon. Not. R. Astron. Soc.* **399**, L128 (2009).
- [8] P. Laurent *et al.*, “A  $14 h^{-3} \text{Gpc}^3$  study of cosmic homogeneity using BOSS DR12 quasar sample,” arXiv:1602.09010 [astro-ph.CO].
- [9] B. Pandey, and S. Sarkar, “Probing large scale homogeneity and periodicity in the LRG distribution using Shannon entropy,” *Mon. Not. Roy. Astron. Soc.* **460**, 1519 (2016).
- [10] J.K. Yadav, J.S. Bagla and N. Khandai, “Fractal dimension as a measure of the scale of homogeneity,” *Mon. Not. Roy. Astron. Soc.* **405**, 2009 (2010).
- [11] F. Sylos Labini, N.L. Vasilyev, L. Pietronero and Y.V. Baryshev, “Absence of self-averaging and of homogeneity in the large scale galaxy distribution,” *Europhys. Lett.* **86**, 49001 (2009).
- [12] F. Sylos Labini and Y.V. Baryshev, “Testing the Copernican and Cosmological Principles in the local universe with galaxy surveys,” *J. Cosmol. Astropart. Phys.* **1006**, 021 (2010).
- [13] F. Sylos Labini, “Inhomogeneities in the universe,” *Classical and Quantum Gravity*, **28**, 164003 (2011).
- [14] C. Park, Y.-Y. Choi, J. Kim, J.R. Gott, S.S. Kim and K.-S. Kim, “The Challenge of the Largest Structures in the Universe to Cosmology”, *Astrophys. J.* **759**, L7 (2012).
- [15] K.N. Abazajian *et al.* [SDSS Collaboration], “The Seventh Data Release of the Sloan Digital Sky Survey,” *Astrophys. J. Suppl.* **182**, 543 (2009).
- [16] D.J. Eisenstein *et al.* [SDSS Collaboration], “Spectroscopic target selection for the Sloan Digital Sky Survey: The Luminous red galaxy sample,” *Astron. J.* **122**, 2267 (2001).
- [17] E.A. Kazin, M.R. Blanton, R. Scoccimarro *et al.*, “The Baryonic Acoustic Feature and Large-Scale Clustering in the Sloan Digital Sky Survey Luminous Red Galaxy Sample,” *Astrophys. J.* **710**, 1444 (2010).
- [18] J. Kim, C. Park, G. Rossi, S.M. Lee and J.R. Gott III, “The New Horizon Run Cosmological N-Body Simulations,” *J. Kor. Astron. Soc.* **44**, 217 (2011).
- [19] S. Alam *et al.* [BOSS Collaboration], “The clustering of galaxies in the completed SDSS-III Baryon Oscillation Spectroscopic Survey: cosmological analysis of the DR12 galaxy sample,” [arXiv:1607.03155 [astro-ph.CO]].
- [20] G. Ellis, “Patchy solutions,” *Nature* **452**, 158 (2008).
- [21] M.R. Calabretta and E.W. Greisen, “Representations of celestial coordinates in FITS,” *Astron. Astrophys.* **395**, 1077 (2002).
- [22] C. Stoughton, R.H. Lupton, M. Bernardi *et al.*, “Sloan Digital Sky Survey: Early Data Release,” *Astron. J.* **123**, 485 (2002).
- [23] K.M. Gorski, E. Hivon, A.J. Banday, B.D. Wandelt, F.K. Hansen, M. Reinecke and M. Bartelman, “HEALPix-A Framework for high resolution discretization, and fast

analysis of data distributed on the sphere," *Astrophys. J.* **622**, 759 (2005).